随焊冲击碾压整形新方法及等承载接头拉伸与疲劳性能

王佳杰[1,2]， 杨建国[3]， 张敬强[1]， 董志波[1]， 方洪渊[1]， 刚 铁[1]

(1. 哈尔滨工业大学 先进焊接与连接国家重点实验室，哈尔滨 150001;
2. 黑龙江工程学院 材料与化学工程学院，哈尔滨 150050; 3. 浙江工业大学 化工机械设计研究所，杭州 310014)

摘 要：提出了随焊冲击碾压整形方法(weld shaping with trailing impact rolling，WSTIR)，并研制了一套随焊冲击碾压整形装置. 对随焊整形后低匹配等承载接头(equal load-carrying capacity，ELCC)进行了拉伸试验和疲劳试验. 结果表明，随焊整形后接头拉伸均断裂在近焊趾的母材处，断裂应力均达到母材的抗拉强度；随焊整形后接头的疲劳寿命明显大于原始焊态接头，由于随焊整形接头焊趾处圆弧过渡降低了应力集中，进而提高了随焊整形接头的疲劳承载能力. 拉伸与疲劳试验说明随焊冲击碾压整形后的平余高低匹配接头达到了等承载的要求. 这种随焊整形方法将有力地推动低匹配等承载接头设计方法在工程实际的应用.

关键词：低匹配对接接头；随焊冲击碾压整形；拉伸性能；疲劳性能
中图分类号：TG404 **文献标识码**：A **文章编号**：0253-360X(2012)11-0035-04

王佳杰

0 序 言

为减小结构厚度和重量，材料不断向高强化方向发展. 同时高强钢焊接时冷裂纹、焊缝韧性不足、热影响区软化和脆化等问题突显出来[1-3]，使得高强钢焊接结构的应用并非尽如人意. 低强匹配接头可以获得塑韧性较好的焊缝，降低冷裂倾向[4,5]，所以低匹配接头已经得到充分的重视. 但是低匹配接头承载能力有所降低. 许多研究人员提出了机械打磨、焊趾TIG熔修、锤击、超声波处理、低相变点焊条熔修等方法[6,7]，确保焊趾区圆滑过渡以降低应力集中，从而提高焊接接头的承载能力. 现已有研究证明[8-11]，通过接头几何形状设计可以提高低匹配接头的承载能力. 对于获得承载接头采用机械加工方法成本高、效率低、强度大等问题，相关文献[12]研究表明冲击杆整形和碾压轮整形分别在一定程度上提高了焊缝的承载能力，但是冲击杆整形只能对单边窄焊缝进行加载，而碾压轮整形可实现一次焊满的盖面焊，不适合多道焊. 文中针对上述焊后机械加工整形与单独一种方式随焊整形的不足，设计了一套随焊冲击碾压联合整形装置，并对随焊整形后等承载接头拉伸和疲劳性能进行了试验研究.

1 随焊整形装置及工作过程

图1为随焊冲击碾压接头整形装置试验平台，主要由压缩空气储气瓶、空气锤、固定支座、冲击碾压整形装置及工作台组成. 其工作过程：储气瓶存满压缩空气，调节气瓶阀门气流量，将空气锤调至轻微震动，此时将引燃TIG电弧，电弧加热接头焊缝表面而不使其熔化，调整工作台按照预定速度行走，再将气瓶气流调整到预定流量，随焊整形开始，当随焊

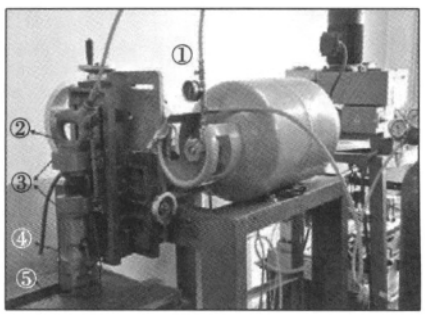

①压缩空气储气瓶 ②气锤 ③固定支座
④冲击碾压整形装置 ⑤工作台

图1 随焊冲击碾压整形试验平台

Fig. 1 Test platform of WSTIR

收稿日期：2012-08-06
基金项目：中俄政府间科技合作资助项目(2007DFR70070)

整形完毕，关闭电弧及气阀.

图 2 为随焊冲击碾压整形装置. 前后碾压轮均由 Gr15 材料制成. 前后碾压轮焊趾半径分别为 8 mm 和 10 mm，前碾压轮深度大于后碾压轮深度，前后碾压轮成形宽度相等.

随焊冲击碾压装置具有结构简单、轻便、可靠、高效，还能够减小劳动强度，有利于等承载接头技术的推广和应用.

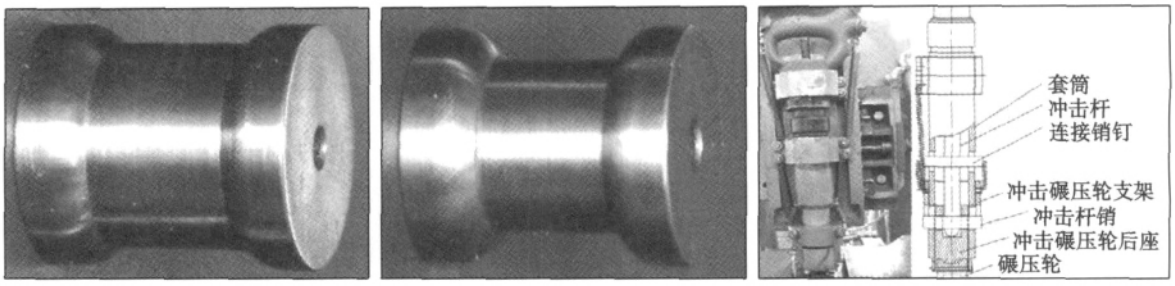

(a) 前碾压轮 (b) 后碾压轮 (c) 整体图

图 2 随焊冲击碾压整形装置

Fig. 2 Device of WSTIR

2 随焊冲击碾压整形装置工作原理

一般认为焊接过程的应力变形是由于被焊工件由于不均匀温度场引起的，在加热过程中焊缝和近缝区的金属热膨胀应变受到周围较冷金属的拘束，从而产生压缩塑性应变. 焊接冷却过程中该压缩塑性应变被拉伸应变抵消一部分，焊后仍有残余压缩塑性应变，从而引起残余变形. 可通过使焊缝产生拉伸塑性应变以抵消、补偿压缩塑性应变，从而减小焊接残余应力变形.

因此依据这种理论，随焊整形装置的工作原理为：钢良好的塑性变形温度区间为 460 ~ 800 ℃ [12]，因此应使随焊整形装置前碾压轮作用于焊缝金属处于此温度区间. 前碾压轮作用在温度高、屈服强度较低和良好塑性变形能力的焊趾处焊缝金属上以及离熔池左右两侧一定距离内的具有较高温度焊缝金属上，通过冲击碾压初步整形获得需要的圆滑过渡焊趾形状及初步获得接头形状；同时后碾压轮紧跟其后对仍具有一定温度的焊缝金属上再进行冲击碾压，以进一步获得所需的接头形状（余高高度、余高宽度和焊趾圆弧过渡半径）并降低焊接残余拉应力、减小焊接变形.

3 试验方法

母材厚度为 8 mm 的 Q620-CF 无裂纹高强钢，开 X 形坡口，采用 E4303 焊条施焊而成，焊接材料性能参数如表 1 所示. 按照等承载要求：焊趾圆弧过渡半径 8 mm、余高高度 4 mm、盖面焊道半宽为 18 mm. 利用随焊整形装置对上述尺寸的接头进行随焊冲击碾压整形. 按照国家标准 GB/T228—2002《金属材料室内拉伸试验方法》对整形后接头制取试样. 拉伸试验采用 CSS40000 万能电子试验机，加载速度为 2 mm/min. 疲劳试验采用 PLG-100C 高频疲劳试验机，平均载荷为 150 MPa，应力比为 0.

表 1 焊接材料性能参数

Table 1 Welding material properties parameters

焊接材料	屈服强度 R_{eL}/MPa	抗拉强度 R_m/MPa	断后伸长率 A(%)
母材金属	629	890	19.2
焊缝金属	365	475	35.6

研究通过 TIG 电弧加热，前碾压轮作用于焊缝金属塑性温度区间，既要保证电弧加热焊缝金属使其具有良好塑性变形能力，同时又要确保焊缝金属软化但不熔化，所以采用小电流摆动，摆动方向垂直于焊缝长度方向，电弧加热参数如表 2 所示.

表 2 TIG 电弧加热参数

Table 2 TIG arc heating parameters

电源类型	钨极直径 D/mm	加热电流 I/A	电弧电压 U/V	移动速度 v/(mm·s^{-1})	保护气体
直流	3.2	100	20	0.5	氩气

4 随焊整形后接头拉伸与疲劳性能

满足等承载要求的低匹配接头随焊冲击碾压整

形后拉伸试样如图 3 所示. 从图 3 可知随焊冲击碾压整形后接头表面较为平整，焊趾部位圆滑半径过渡. 随焊冲击碾压整形后拉伸试验结果如图 4 和表 3 所示，断裂应力是按照母材的平均应力计算. 在普通余高削平的低匹配对接焊接接头中，断裂位置总会发生在低匹配的焊缝金属上. 按等承载原则设计的随焊冲击碾压整形后平余高低匹配焊接接头拉伸结果表明，所有低匹配焊接接头均断裂于近焊趾的母材处，断裂应力均达到母材的抗拉强度，说明随焊冲击碾压整形后的平余高低匹配焊接接头满足静载拉伸等承载的要求.

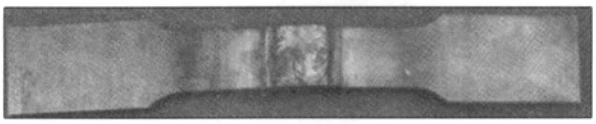

图 3　等承载接头随焊整形后拉伸试样

Fig. 3　Tensile specimen of ELCC joints after WSTIR

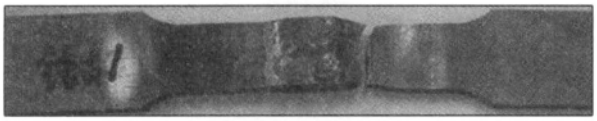

图 4　等承载接头随整形后拉伸效果

Fig. 4　Tensile test effect of ELCC joints after WSTIR

表 3　等承载接头随整形后拉伸试验结果

Table 3　Tensile test results of ELCC joints after WSTIR

试件编号	抗拉强度 R_m/MPa	断裂位置
L1	886	近焊趾母材
L2	897	近焊趾母材
L3	889	近焊趾母材
L4	900	近焊趾母材
L5	891	近焊趾母材

疲劳性能也是工程中比较关心的问题. 为更清楚的说明随焊整形接头的疲劳性能效果，比较了相同疲劳载荷下原始焊态对接接头与随焊整形后接头的疲劳性能. 两种接头的焊趾形状如图 5 所示. 显然由图 5 可知，随焊冲击碾压整形后的接头焊趾处存在圆弧过渡，焊趾过渡半径明显增大，而原始焊态接头焊趾处不存在圆弧过渡.

疲劳试验结果如表 4 所示. 结果表明，无论是原始焊态接头，还是随焊整形接头，所有接头都断裂在焊趾处. 总的来说，随焊整形接头的疲劳寿命明显大于原始焊态接头，这是由于随焊整形接头焊趾处存在一定的圆弧过渡，焊趾处的应力集中在一定

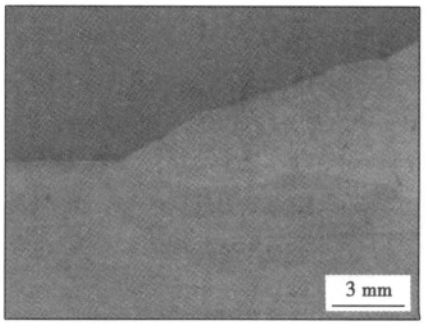

(a) 原始焊态接头

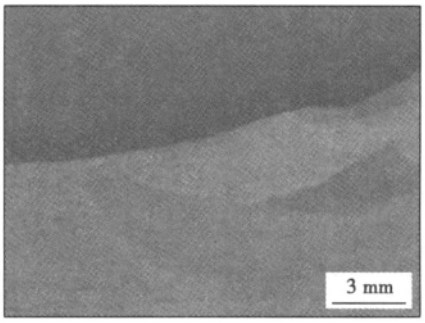

(b) 随焊整形后接头

图 5　接头焊趾形状

Fig. 5　The shape of the weld toe

程度上得到降低，进而提高了随焊整形接头的疲劳承载能力. 等承载接头在焊接和试样下料过程中使焊趾处残余应力发生改变，以及焊缝在随焊整形过程中在焊趾处引入残余应力等多种因素综合作用的结果，关于残余应力对等承载接头疲劳性能的影响还有待于进一步研究.

表 4　两种接头疲劳试验结果

Table 4　Fatigue test results of two kinds of joints

接头类型	试件编号	循环周次 $N/10^5$ 次	平均循环周次 $\bar{N}/10^5$ 次	断裂位置
随焊整形	Z1	1.658 79	1.848 19	焊趾
	Z2	2.034 79		焊趾
	Z3	2.156 83		焊趾
	Z4	1.572 49		焊趾
	Z5	1.818 08		焊趾
原始焊态	H1	0.998 15	1.684 73	焊趾
	H2	1.105 63		焊趾
	H3	1.347 25		焊趾
	H4	0.987 42		焊趾
	H5	1.985 23		焊趾

综上所述，按照等承载要求的具有形状参数平余高低匹配接头随焊冲击碾压整形后的接头拉伸试验与疲劳试验仍满足等承载的要求，达到了预期的整形效果. 这种随焊整形方法将会有力地推动低匹

配等承载接头设计方法在工程实际的应用.

5 结 论

(1) 提出了随焊冲击碾压整形的新方法,并研制出一整套应用于平余高对接接头的随焊冲击碾压整形装置,结构简单、轻便、可靠、高效,还能够减小劳动强度,有利于等承载接头技术的推广和应用.

(2) 拉伸结果表明,随焊整形后平余高低匹配焊接接头拉伸均断裂于近焊趾的母材处,抗拉强度均达到母材的抗拉强度,说明随焊整形后的平余高低匹配焊接接头满足静载拉伸等承载的要求.

(3) 疲劳试验结果表明,随焊整形接头的疲劳寿命明显大于原始焊态接头,由于随焊整形接头焊趾处的圆弧过渡降低了应力集中,进而提高了随焊整形接头的疲劳承载能力.

参考文献:

[1] Magudeeswaran G, Balasubramanian V, Madhusudhan G. Effect ofwelding processes and consumables on high cycle fatigue life of high strength quenched and tempered steel joints [J]. Materials and Design, 2008, 29: 1821-1827.

[2] Magudeeswaran G, Balasubramanian V, Madhusudhan G. Hydrogeninduced cold cracking studies on armour grade high strength [J]. International Journal of Hydrogenenergy, 2008, 33: 1897-1908.

[3] 杨建国, 黄鲁永, 张 勇,等. 30CrMnSi 钢 TIG 焊冷裂纹形成机制 [J]. 焊接学报, 2011, 32(12): 13-16.
Yang Jianguo, Huang Luyong, Zhang Yong, *et al*. Mechanism of cold welding cracks in 30CrMnSi steel joints welded by TIG method [J]. Transactions of the China Welding Institution, 2011, 32(12): 13-16.

[4] Irving B U S. Navy maintains high interest in funding for welding research [J]. Welding Journal, 1995, 74(3): 41-47.

[5] KimY J, Schwalbe K H. Numerical analyses of strength mismatch effect on local stresses for ideally plastic materials [J]. Engineering Fracture Mechanics, 2004, 71: 1177-1199.

[6] Kirkhope K J, Bell R, Caron L. Weld detail fatigue life improvement techniques, part 1 review [J]. Marine Structures, 1999, 12: 447-474.

[7] Sonsino C M. Fatigue life improvement of welded structures by post-weld treatments and some limitations by geometry and loading mode [J]. Revue de Metallurgie, 2007, 104(1): 51-57.

[8] 赵智力, 方洪渊, 杨建国, 等. 一种针对低匹配焊接接头的"等承载"设计方法 [J]. 焊接学报, 2011, 32(4): 87-90.
Zhao Zhili, Fang Hongyuan, Yang Jianguo, *et al*. A design method of equal load-carrying capacity for under-matching weld joints [J]. Transactions of the China Welding Institution, 2011, 32(4): 87-90.

[9] 王佳杰, 董志波, 刘雪松, 等. 弹性阶段低匹配对接接头三点弯曲余高形状设计 [J]. 焊接学报,2012, 33(8): 37-40.
Wang Jiajie, Dong Zhibo, Liu Xuesong, *et al*. Shape design of the reinforcement for under-matched butt joints under the three-point bending load in elastic stage [J]. Transactions of the China Welding Institution, 2012, 33(8): 37-40.

[10] 王 涛, 杨建国, 刘雪松, 等. 含中心裂纹低匹配对接接头形状参数对形状因子的影响 [J]. 焊接学报, 2012, 33(1): 101-104.
Wang Tao, Yang Jianguo, Liu Xuesong, *et al*. Iinfluence of joint geometric parameters on shape factor of under-matched butt joint with center crack [J]. Transactions of the China Welding Institution, 2012, 33(1): 101-104.

[11] Wang Tao, Yang Jianguo, Liu Xuesong, *et al*. Stress intensity factor expression for center-cracked butt joint considering the effect of joint shape [J]. Materials and Design, 2012, 35: 72-79.

[12] 周立鹏. 低匹配等承载对接接头随焊整形可行性研究 [D]. 哈尔滨: 哈尔滨工业大学, 2011.

作者简介: 王佳杰,男,1975 年出生,博士研究生,副教授. 主要从事焊接结构可靠性分析和热喷涂技术教学与科研工作. 发表论文 20 余篇. Email: wangjiajie2006@126.com.

通讯作者: 杨建国,男,副教授,博士. Email: yangjg@zjut.edu.cn

remelted sample had higher hardness, better wear resistance than the as-sprayed coating.

Key words: laser remelting; plasma spraying; Ni-based coating; WC particles reinforced

Parametric modeling and vector graphics plotting for welding joint groove SHEN Chunlong[1,2], YU Jingbao[2], PENG Yong[2], WANG Kehong[2] (1. Dept. Mechanical & Electrical Engineering, Taizhou Teacher College, Taizhou 225300, China; 2. School of Material Science & Engineering, Nanjing University Science & Technology, Nanjing 210094, China). pp 17-20

Abstract: Parametric description and graphics plotting of welding joint groove play an important role for software development of welding process design. Parametric model of joint type and groove graphics is presented based on double U-groove. Principle for joint groove graphics parameter-driven is analyzed and the function of geometry parameter dynamic labeling for groove graphics is realized. The classes for primitives plotting object-oriented are presented. The primitives-data storage structure of parameter plotting process is showed. The use of picking primitive object with mouse resolves the question of modifying the primitive properties. The generation of neutral vector WMF file and serialization process for joint graphics are discussed. The results show that parametric model and vector plotting for joint groove graphics can handle labeling for joint parameter and embed graphics distortion in report form.

Key words: joint groove; parametric modeling; vector graphics; parameter-driven

Effect of premelting oxide layer on AA-TIG weld shape FAN Ding[1,2], KANG Zaixiang[2], HUANG Yong[1,2], Yan Liqin[2], WANG Xinxin[2], HAO Zhenni[2] (1. State Key Laboratory of Gansu Advanced Non-ferrous Metal Materials, Lanzhou University of Technology, Lanzhou 730050, China; 2. Key Laboratory of Non-ferrous Metal Alloys, The Ministry of Education, Lanzhou University of Technology, Lanzhou 730050, China). pp 21-25

Abstract: AA-TIG welding is a new and efficient welding process before which pre-melting oxide layer was prepared on weld position by low current assisting arc with $Ar+O_2$ as shield gas. As a result, a deep and narrow weld bead can be obtained. In this experiment, through turning the assisting arc parameters to change the thickness of oxide layer, the influence of the thick of oxide layer on stainless steel weld formation was analyzed. The results show that the parameters of assisting arc have great effect on the thickness of oxide layer, the oxide layer becomes thicker when the oxygen gas flow rate or the heat input of assisting arc increase. And the thickness of oxide layer influences the weld depth/width ratio, the weld depth/width ratio climbs up at first and then declines with the increase of the thickness of oxide layer.

Key words: stainless steel; AA-TIG welding; oxide layer; weld shape

Effect of temperature on CO_2 corrosion of dissimilar weld joint WANG Jing[1], LU Minxu[1], YANG Ping[1], ZHANG Lei[1], CHANG Wei[2] (1. School of Materials Science and Engineering, University of Science and Technology Beijing, Beijing 100083, China; 2. China National Offshore Oil Corp. (CNOOC) Research Center, Beijing 100027, China). pp 26-30

Abstract: To study the effect of temperature on CO_2 corrosion behavior of dissimilar weld joint, dissimilar weld joint of X70 pipeline steel and 2250 duplex stainless steel welded by metal inertia gas welding was used experimentally. Microstructure of X70/weld joint interface and CO_2 corrosion morphologies in weld joint at different temperatures were observed and analyzed. The results showed that dendritic structure appeared in weld joint. Narrow fusion zone and type Ⅱ boundary existed between micro-alloy steel and weld joint, and obvious concentration gradient of Ni and Cr elements was observed. Serious corrosion occurred in HAZ of micro-alloy at high temperature other than at low temperature. Corrosion product on surface of micro-alloy was shown loose while that on surface of weld joint was shown compact. Such different corrosion tendency of micro-alloy and weld joint was probably caused by the different ionic migration ratios as a result of different corrosion potentials of metals and different temperatures.

Key words: temperature; dissimilar weld joint; microstructure; corrosion rate; mechanism

Weld appearance behavior in welding pool of stainless steel by ultrahigh frequency pulse GTAW process YANG Mingxuan[1], QI Bojin[1], CONG Baoqiang[1], LI Wei[1,2], YANG Zhou[1] (1. School of Mechanical Engineering and Automation, Beihang University, Beijing 100191, China; 2. Beijing Institute of Petrochemical Technology, Beijing 100191, China). pp 31-34

Abstract: Based on ultrahigh frequency pulse gas tungsten arc welding process for stainless steel, appearance of weld and the influence of pulse current to flow in welding pool were carried out. The experimental results show that the welds penetration increased with the increasing of pulse frequency. When the pulse frequency $f=80$ kHz, the weld penetration rose by 24.6% at least with the depth increased by 88.7% at most. It could also be found that the width and depth of weld had the similar trend with the changed pulse frequency. Based on the data from experiments, the flow movement in the pool was investigated with effect of electromagnetic force to weld appearance and forced flow as the main purpose.

Key words: ultrahigh frequency pulse GTAW process; appearance of weld; flow behavior of welding pool

A new weld shaping method with trailing impact rolling and tensile and fatigue properties for equal load-carrying capacity joints WANG Jiajie[1,2], YANG Jianguo[3], ZHANG Jingqiang[1], DONG Zhibo[1], FANG Hongyuan[1], GANG Tie[1] (1. State Key Laboratory of Advanced Welding and Joining, Harbin Institute of Technology, Harbin 150001, China; 2. School of Materials and Chemical Engineering, Heilongjiang Institute of Technology, Harbin 150050, China; 3. Institute of Process Equipment and Control Engineering, Zhejiang University of Technology, Hangzhou 310014, China). pp 35-38

Abstract: A new modified technology is put forward in which weld shaping with trailing impact rolling is used (WSTIR). The integrated device of WSTIR has also been designed. Tensile test and fatigue test has been carried out respectively for under-matched equal load-carrying capacity joints after modifying. Tensile test results show that tensile fracture occurs in the base metal near the weld toe and tensile strength reaches the tensile strength of base metal for equal load-carrying capacity joints after WSTIR. Fatigue test results show that the fatigue life of equal load-carrying capacity joints after WSTIR is significantly greater than the original welded joints. The weld toe arc transition can reduce stress concentration, thereby improve fatigue carrying capacity of WSTIR joints. The results of tensile and fatigue test show that the modified flat-reinforcement joints have the same load carrying capcity with base metal. This shaping method with WSTIR will greatly promote the practical application in engineering for the undermatching equal load-carrying capacity joints.

Key words: undermatching welded joints; weld shaping with trailing impact rolling; tensile property; fatigue property

Effect of Ni on interfacial IMC and mechanical properties of Sn2.5Ag0.7Cu0.1RE/Cu solder joints LI Chenyang[1], ZHANG Keke[1], WANG Yaoli[1], ZHAO Kai[1], DU Yile[2] (1. Material Science & Engineering College, Henan University of Science & Technology, Luoyang 471003, China; 2. Luo Yang Ruichang Petro-Chemical Equipment Co., Ltd, Luoyang 471003, China). pp 39-42

Abstract: The effects of Ni on the microstructure and mechanical properties of Sn2.5Ag0.7Cu0.1RE solder and solder joints were studied by using the scanning electronic microscope and X-ray diffraction. The results show that adding proper amount of Ni in Sn2.5Ag0.7Cu0.1RE solder alloys can refine the initial β-Sn phase and eutectic structure, suppress the growth of the $(Cu,Ni)_6Sn_5$ intermetallic compound (IMC) at the interface of solder joints, and reduce the roughness of interfacial IMC, improve the shear strength of the SnAgCuRE/Cu solder joints. The solder alloy structure was fine and homogenous, eutectic structure proportion was large, interfacial IMC was thin and flat and the grain size of (Cu,Ni)6Sn5 was small. The shear strength got the maximum value (45.6 MPa) when the Ni content was 0.1 wt%, which was 15.2% higher than the solder joints without Ni.

Key words: Sn2.5Ag0.7Cu0.1RExNi solder alloys, solder joints; intermetallic compound(IMC); mechanical properties

Microstructure and abrasion resistance of high-chromium open arc hardfacing alloys GONG Jianxun, XIAO Yifeng (School of Mechanical Engineering, Xiangtan University, Xiangtan 411105, China). pp 43-46, 50

Abstract: Wear-resisting alloys containing Cr 21% ~ 23%, C 3.5% ~ 4.2%, Si 1.4% ~ 1.6%, B 0% ~ 1.8% (mass fraction) were deposited by metal powdered-type flux-cored wire self-shielded open arc welding. The effects of B4C content in flux-cored wire on the microstructure and abrasion resistance as well as the solidifying characteristics of weld puddles and the effects of Si, B on the deoxidization of weld beads were studied by the methods of optical microscopy (OM), X-ray diffraction (XRD), scanning electron microscopy (SEM) and energy dispersive spectrometer (EDS). It shows that Si_5C_3 can act as a good homogeneous nucleate core of primary M_7C_3 grain. With the addition of B_4C particles, the volume fraction and the size of primary M_7C_3 grains increase remarkably and their morphology changes from dispersion to aggregation. In addition, the results of wet sand rubber wear tests and the analysis of worn morphology indicate that abrasion resistance depends on the size and the morphology of primary M_7C_3 grains and micro-spalling is the dominating wear mechanism.

Key words: open arc; high chromium; hardfacing; abrasion resistance; microstructure

Interfacial structure and strength of Si_3N_4 ceramics joint brazed with amorphous filler metal and Cu layer ZOU Jiasheng, ZENG Peng, XU Xiangping (Provincial Key Lab of Advanced Welding Technology, Jiangsu University of Science and Technology, Zhenjiang 212003, China). pp 47-50

Abstract: Si_3N_4 ceramics was brazed with TiZrCuB amorphous filler metal and Cu interlayer, the effect of brazing metal composition and thickness of copper foil on interfacial structure and bonding strength were studied in this paper. The result shows that the joint strength is up to 241 MPa when the brazing temperature is 1 323 K, holding time is 30min, the thickness of Cu interlayer is 70 m and the exerted pressure is 0.027 MPa. the reaction layer is TiN, the interface microstructure is compounds of Si_3N_4/TiN/Ti-Si+Ti-Zr+Cu-Zr+α-Cu; changing the thickness of interlayer can adjust the thickness and composition of the reaction layer; As the thickness of Cu interlayer increases, Ti-Si compound layer has gradually separated from the TiN layer, and it is pushed to the weld center and refined to a granula shape.

Key words: amorphous brazing filler metals; Cu interlayer; Si_3N_4 ceramics; interfacial structure; bonding strength

Diffusion bonding joint of TiAl-based alloy and Ni-based alloy by using composite interlayer LI Haixin, LIN Tiesong, HE Peng, FENG Jicai, WANG Xianjun (State Key Laboratory of Advanced Welding and Joining, Harbin Institute of Technology, Harbin 150001, China). pp 51-54

Abstract: Diffusion bonding of TiAl-based alloy to Ni-based alloy by using Ti/Nb and Ti/Nb/Ni composite interlayer was carried out. The interfacial microstructure and fracture morphology were investigated by scanning electron microscopy and electron probe X-ray microanalysis. The bonding strength of the joints was evaluated through shear test. The results showed that when the interlayer was Ti/Nb, the optimum bonding time was t = 30 min, the maximum shear strength was R_τ = 273.8 MPa, and the fracture occured at the GH99/Nb interface; when the interlayer was Ti/Nb/Ni, the optimum bonding time was t = 60 min, the maximum shear strength was R_τ = 314.4 MPa, the frac-